

# SCIENTIFIC REPORTS



OPEN

## Critical Role of COI1-Dependent Jasmonate Pathway in AAL toxin induced PCD in Tomato Revealed by Comparative Proteomics

Received: 27 April 2016

Accepted: 31 May 2016

Published: 21 June 2016

Min Zhang<sup>1,\*</sup>, Jin Koh<sup>2,\*</sup>, Lihong Liu<sup>1,3,\*</sup>, Zhiyong Shao<sup>1</sup>, Haoran Liu<sup>1</sup>, Songshen Hu<sup>1</sup>, Ning Zhu<sup>3</sup>, Craig P. Dufresne<sup>4</sup>, Sixue Chen<sup>2,3</sup> & Qiaomei Wang<sup>1,5</sup>

*Alternaria alternata* f.sp. *Lycopersici* (AAL) toxin induces programmed cell death (PCD) in susceptible tomato (*Solanum lycopersicum*) leaves. Jasmonate (JA) promotes AAL toxin induced PCD in a COI1 (coronatine insensitive 1, JA receptor)-dependent manner by enhancement of reactive oxygen species (ROS) production. To further elucidate the underlying mechanisms of this process, we performed a comparative proteomic analysis using tomato *jasmonic acid insensitive1* (*jai1*), the receptor mutant of JA, and its wild type (WT) after AAL toxin treatment with or without JA treatment. A total of 10367 proteins were identified in tomato leaves using isobaric tags for relative and absolute quantitation (iTRAQ) quantitative proteomics approach. 2670 proteins were determined to be differentially expressed in response to AAL toxin and JA. Comparison between AAL toxin treated *jai1* and its WT revealed the COI1-dependent JA pathway regulated proteins, including pathways related to redox response, ceramide synthesis, JA, ethylene (ET), salicylic acid (SA) and abscisic acid (ABA) signaling. Autophagy, PCD and DNA damage related proteins were also identified. Our data suggest that COI1-dependent JA pathway enhances AAL toxin induced PCD through regulating the redox status of the leaves, other phytohormone pathways and/or important PCD components.

Fungi usually produce toxins to damage plant tissues, which are classified as host-selective or non-specific. Host-selective toxins (HSTs) only infect host plants, but non-specific toxins can infect plants whether they are a host or non-host of fungus producing pathogen<sup>1</sup>. *Alternaria alternata* f.sp. *Lycopersici* (AAL) toxin is a kind of HST, it is the main virulence effector produced by AAL, causing stem canker and leaf necrosis on tomato (*Solanum lycopersicum*) plants of the *asc/asc* genotype<sup>2,3</sup>, leading to serious crop loss. The recessive allele (*asc/asc*) is associated with a mutation in the single codominant *Alternaria Stem Canker* (ASC) gene, which determines the insensitivity of plants to fungal AAL<sup>4</sup>. AAL toxin is one type of sphinganine analogue mycotoxins (SAMs) that are inhibitors of eukaryotic sphinganine N-acyltransferase (acyl-CoA-dependent ceramide synthase), a key enzyme in the sphingolipid ceramide biosynthetic pathway<sup>5</sup>. The disruption of sphingolipid biosynthesis causes marked elevation of free sphingoid bases such as phytosphingosine and sphinganine<sup>6</sup>, which triggers programmed cell death (PCD) in susceptible plant cells<sup>7</sup>. Among the five series (TA, TB, TC, TD, and TE) of AAL toxin, TA is the most common kind of AAL toxin<sup>8</sup>. As an active and controlled cell death essential for plant defense, PCD functions in diverse biological processes that are related to the complicated network of PCD development<sup>9</sup>. However, the role and regulatory mechanisms of PCD in plants are still poorly understood.

During host-pathogen interactions, jasmonate (JA) and ethylene (ET) are associated with defense against necrotrophic pathogens, while salicylic acid (SA) plays a major role in activation of defense against biotrophic pathogens<sup>10</sup>. Several studies showed that JA and ET are closely related to AAL toxin induced PCD<sup>11</sup>. During

<sup>1</sup>Key Laboratory of Horticultural Plant Growth, Development and Quality Improvement, Ministry of Agriculture, Department of Horticulture, Zhejiang University, Hangzhou 310058, China. <sup>2</sup>Proteomics and Mass Spectrometry, Interdisciplinary Center for Biotechnology Research, University of Florida, Gainesville, FL 32610, USA. <sup>3</sup>Department of Biology, Genetics Institute, University of Florida, Gainesville, FL 32610, USA. <sup>4</sup>Thermo Fisher Scientific, West Palm Beach, Florida 33407, USA. <sup>5</sup>Zhejiang Provincial Key Laboratory of Horticultural Plant Integrative Biology, Department of Horticulture, Zhejiang University, Hangzhou 310058, China. <sup>\*</sup>These authors contributed equally to this work. Correspondence and requests for materials should be addressed to Q.W. (email: qmwang@zju.edu.cn)

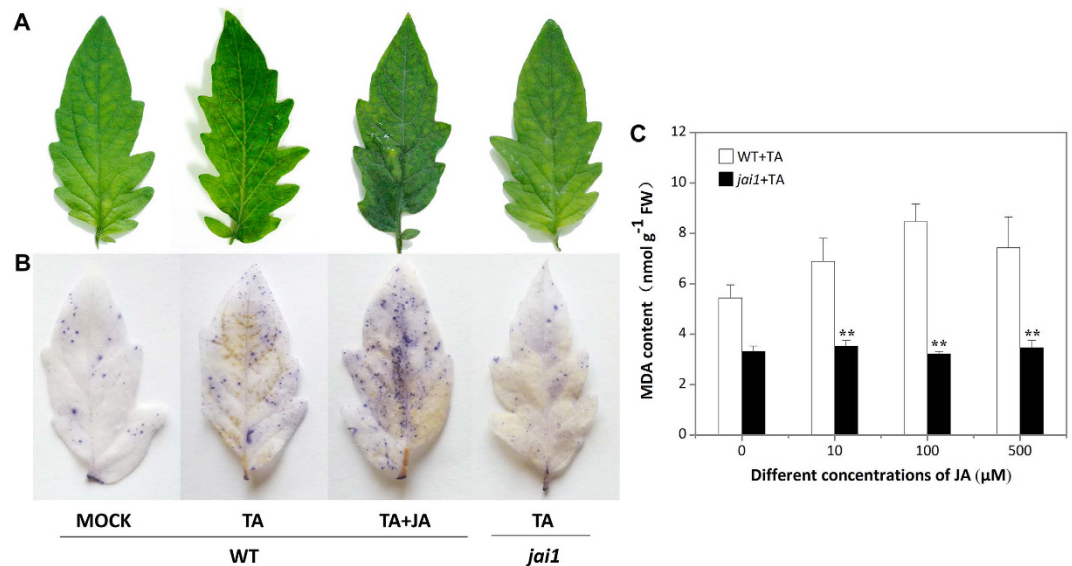


**Figure 1.** Effect of JA pathway on TA induced PCD in detached tomato leaves. Detached leaflets were incubated under continuous light at 25 °C for 48 h. WT, wild type; *jai1*, JA receptor mutant; Mock, WT leaves treated with SPB buffer; TA, WT or *jai1* leaves treated with TA; TA + JA, WT or *jai1* leaves treated with TA and JA. (A) Fully expanded leaflets from nodes between fourth to sixth of 7-week-old plants were treated with 0.2 μM TA with or without 100 μM JA and photographed after 48 h. (B) Leaves from WT and *jai1* plants were stained with trypan blue for the degree determination of dead and dying cells after treatment for 48 h. (C) MDA content was detected in WT and *jai1* leaflets after co-treated with different concentrations of JA (0, 10, 100, and 500 μM) and 0.2 μM TA for 48 h. Each data point represents the mean of three replicates. Error bars indicate standard deviation of three replicates, asterisks above the bars indicate statistically significant differences between different treatments, as determined by the Student *t*-tests (\*\**P* < 0.01).

AAL toxin induced PCD process in *Arabidopsis loh2* mutant (a T-DNA knockout mutant of a homologue of the tomato *Asc* gene), ET-responsive genes were up-regulated within seven hours, but JA pathway related genes were unchanged, and there was no indication of JA accumulation<sup>12</sup>. Egusa *et al.*<sup>13</sup> reported that methyl-jasmonic acid (MeJA) has a promotional effect on susceptibility of tomato to AAL, suggesting that pathogen might utilize JA signaling pathway for successful infection. Moreover, our previous study showed that JA and ET promoted AAL toxin induced cell death alone, and the receptor-dependent JA signaling promotes PCD through enhancing ET biosynthesis<sup>11</sup>. *jai1* (*jasmonic acid insensitive1*) contains a mutation in the tomato homologue of *Arabidopsis COI1* and fails to express JA-regulated genes in response to wounding and MeJA<sup>14</sup>. Hence, the system of AAL toxin and its susceptible tomato host is an excellent model for studying PCD in pathogen response pathways, as the PCD process can be evaluated in a system absence of pathogen, which greatly simplifies the analysis. Besides, the *jai1* mutant allows us to conduct an extensive study in the role of JA pathway in AAL toxin induced PCD.

Reactive oxygen species (ROS) are well known as toxic metabolic substance that can initiate PCD in plant<sup>15</sup>. In *Arabidopsis*, the responses of the JA signaling mutants *jar1* and *fad3/7/8* to O<sub>3</sub> have indicated that JA could be an important factor involved in the ROS-dependent lesion propagation<sup>16</sup>, hence it is quite interesting to investigate the relationship between ROS and JA pathway during AAL toxin induced PCD.

Although large scale transcriptome analysis has deepened our understanding of the molecular basis of toxin induced PCD, proteomics is another powerful tool to further reveal the regulatory and metabolic pathways underlying plant development and response to stresses<sup>17,18</sup>. In this study, we investigated whether JA promoted AAL toxin induced PCD in a COI1-dependent way, and ROS acted downstream of JA in this process. In addition, a comparative proteomics analysis was performed on AAL toxin treated *jai1* mutant and its WT. The data revealed that JA pathway promoted AAL toxin induced PCD by regulating the ROS status of the leaves and relevant PCD components and/or through other hormone pathways in a COI1-dependent manner.

## Results

**COI1-dependent jasmonate pathway promotes TA induced cell death.** The visible necrotic lesions were observed at 36 h in leaves of WT plants after TA treatment (data not shown), and the lesions became typical at 48 h. The PCD symptom was enhanced dramatically in WT leaves when treated with TA and JA together in comparison with TA treatment alone (Fig. 1A), suggesting that JA can promote TA induced PCD. Nevertheless, TA treated *jai1* leaves displayed minor tissue damage at 48 h, and exogenous JA did not exert effect on it, indicating that COI1 is involved in the PCD process triggered by TA and the impaired JA perception in *jai1* inhibited JA promoted PCD.

Trypan blue staining is an accepted method for cell viability assay, live cells or tissues with intact cell membranes are not coloured, and dead cells can be colored in light blue<sup>19</sup>. As can be seen in Fig. 1B, TA treated WT leaves accumulate more blue precipitate compared with the control, and JA enhanced the accumulation of blue

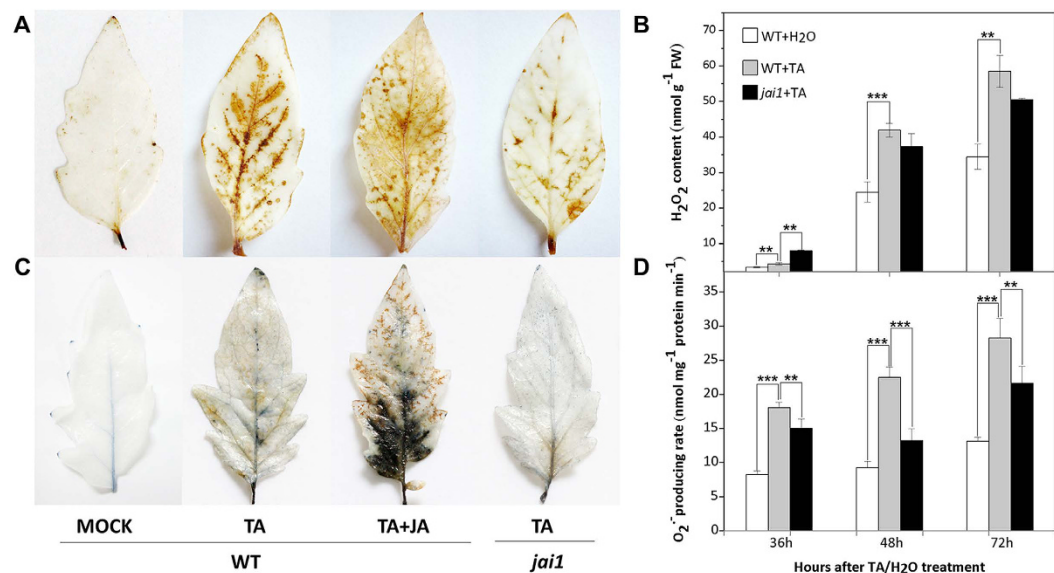


**Figure 2. Effect of JA pathway on TA induced ROS accumulation in detached tomato leaves.** WT, wild type; *jai1*, JA receptor mutant; Mock, WT leaves treated with SPB buffer; TA, WT or *jai1* leaves treated with TA; TA + JA, or *jai1* leaves treated with TA and JA. (A) Leaves of WT and *jai1* were stained with DAB for H<sub>2</sub>O<sub>2</sub> determination at 48 h after 0.2 μM TA treatment with or without 100 μM JA. (B) Changes of H<sub>2</sub>O<sub>2</sub> content in WT and *jai1* leaves after 0.2 μM TA treatment for 36, 48 and 72 h. (C) Leaves of WT and *jai1* were stained with NBT for O<sub>2</sub><sup>-</sup> determination at 48 h after 0.2 μM TA treatment with or without 100 μM JA. (D) Changes of O<sub>2</sub><sup>-</sup> producing rate in WT and *jai1* leaves after 0.2 μM TA treatment for 36, 48 and 72 h. Each data point represents the mean of three replicates. Error bars indicate standard deviation of three replicates, asterisks above the bars indicate statistically significant differences between different treatments, as determined by the Student *t*-tests (\*\**P* < 0.01, \*\*\**P* < 0.001).

precipitate, indicating that JA can promote TA induced PCD. Besides, TA treated *jai1* leaves accumulated less blue precipitate compared with TA treated WT leaves, which was consistent with the visible phenotype (Fig. 1A), further proved that JA pathway is important for TA induced PCD.

Malondialdehyde (MDA) is the final product of membrane lipid peroxidation, which can be a marker for oxidative stress<sup>20</sup>. MDA content in TA treated WT leaves increased with the increase in JA concentration, and peaked at 100 μM JA. However, no visible change was found in *jai1* leaves with the increase in JA concentration (Fig. 1C), indicating that JA enhanced membrane lipid peroxidation in a COI1-dependent way.

**JA enhances ROS accumulation during TA induced PCD.** Hydrogen peroxide (H<sub>2</sub>O<sub>2</sub>) and superoxide (O<sub>2</sub><sup>-</sup>) are the two key ROS molecules. We carried out histochemical 3,3'-diaminobenzidine (DAB)<sup>21</sup> and nitro blue tetrazolium (NBT) staining<sup>22</sup> to detect H<sub>2</sub>O<sub>2</sub> and O<sub>2</sub><sup>-</sup> in the leaves, respectively. As shown in Fig. 2A, after TA treatment for 48 h, large brown precipitation was observed to be around the leaf veins of WT plants by DAB staining, and the brown region was expanded by JA treatment. However, *jai1* leaves showed little precipitation after TA treatment, suggesting less ROS production in *jai1*. The H<sub>2</sub>O<sub>2</sub> content in WT and *jai1* leaves increased steadily during three days with TA treatment, whereas in *jai1* it was significantly lower than WT leaves, except for 36 h after treatment (Fig. 2B). Similarly, much more blue precipitates in TA and JA treated WT leaves was observed than in *jai1* leaves by NBT staining (Fig. 2C). O<sub>2</sub><sup>-</sup> production rate in WT and *jai1* leaves both increased constantly in three days after TA treatment, but it was significantly lower in TA treated *jai1* compared with WT leaves at the same time point (Fig. 2D). Based on these results, it is proposed that ROS burst occurs during TA induced PCD, and the impairment of COI1 suppresses the production of ROS, as well as the necrotic cell death. In Fig. 2B,D, H<sub>2</sub>O<sub>2</sub> content and O<sub>2</sub><sup>-</sup> production rate in the untreated leaves were also increased slightly, possibly caused by the minor stress brought by the treatment.

**Proteome profiling of tomato leaves.** To better understand the mechanisms in TA response of tomato leaves and how JA influences the process, a comparative proteomic analysis was performed in JA insensitive mutant *jai1* and its WT after TA treatment with or without JA treatment. We employed high-resolution MS in combination with isobaric tags for relative and absolute quantitation (iTRAQ) proteomics approach to identify the proteome changes. In our workflow, there are four biological replicates for each treatment and one set of iTRAQ includes two biological replicates (Fig. 3A). We identified a total of 8501 tomato proteins with 1% global false discovery rate (FDR) (Supplementary Figure S1) and 10367 tomato proteins with 5% FDR (Fig. 3B), and the 10367 proteins were chosen for the subsequent analysis.

**Functional classification of the 10367 proteins.** The identified proteins were analyzed based on the assigned functions of the proteins using Uniprot, NCBI and phytozome databases. The biological process of the overall 10367 proteins were classified into 36 categories sorted by the Blast2Go level 4 (Fig. 3D), among them

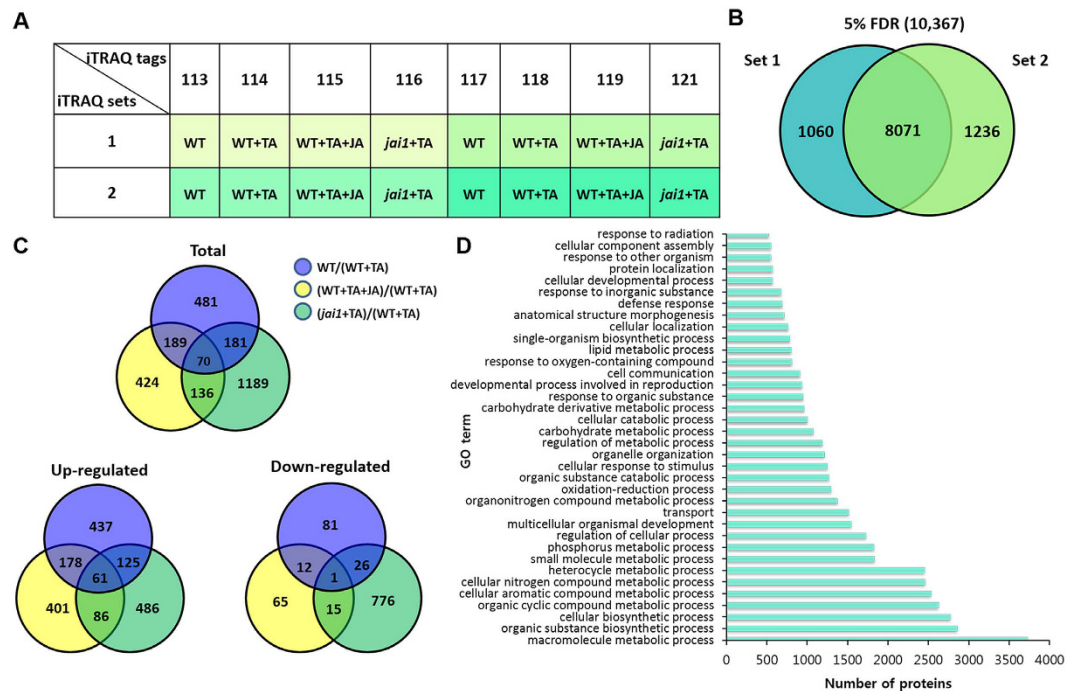


**Figure 3. Comparative proteomics identified a large number of proteins involved in TA induced PCD.** (A) Label by iTRAQ reagent. WT refers to the wild type leaves as control; WT + TA, WT leaves treated with TA; WT + TA + JA, WT leaves treated with TA and JA together; *jai1* + TA, *jai1* leaves treated with TA. Four biological replicates for each treatment and one set of iTRAQ includes two biological replicates. (B) Total protein number identified in two sets with 5% false discovery rate (FDR), set 1 is colored in blue, set 2 is colored in green. (C) Distribution and overlap of differentially expressed (DE) proteins in each comparison. WT + TA was set as the control group for the other groups. Each color represents one contrast. Blue, WT vs WT + TA; Yellow, WT + TA + JA vs WT + TA; Green, *jai1* + TA vs WT + TA. (D) GO terms distribution of the overall 10367 proteins categorized in “biological process”. GO-terms were categorized by Blast2Go at level 4 according to their corresponding GO-term (biological process). Each protein may be identified in more than one process.

most proteins were involved in macromolecule metabolic process (36%), organic substance biosynthetic process (28%) and cellular biosynthetic process (27%), regulation of cellular process (17%), oxidation-reduction process (12%) and cellular response to stimulus (12%). Interestingly, there were 9% proteins involved in cell communication, 8% proteins involved in the lipid metabolic process, 7% proteins involved in the defense response, other proteins were involved in transport (15%), organelle organization (12%), developmental process including reproduction (9%) and anatomical structure morphogenesis (7%).

**Subcellular localization of the 10367 proteins.** The identified proteins were further classified according to their sub-cellular localization (Supplementary Figure S4). As shown in the graph, the proteins were mainly located in nucleus and chloroplast (both 16%), followed by cytosol, mitochondrion and membrane (above 8%), cytoplasm (7%), plasma membrane (6%), golgi (6%), vacuole (4%), ribosome (3%), cell wall (3%) and so on, while 7% had no specified sub-cellular localization. Significantly, the percentage of proteins located in plasmodesma is 2%, this location may indicated the communication between cells.

**Functional annotation and KEGG pathway analysis of the 10367 proteins.** The Kyoto Encyclopedia of Genes and Genomes (KEGG) is a collection of pathways for understanding high-level functions and utilities of the biological system from genomic and molecular-level information<sup>23</sup>. We conducted KEGG pathway analysis of the identified proteins. The proteins were mapped to a total of 139 maps (pathways with more than 40 sequences were represented in Table 1, the others were represented in Supplementary Table S5). The proteins were annotated in various pathways relevant to the synthesis, metabolism or degradation of nucleotide (12%), amino acid (22%), carbohydrate (6%), lipid (14%), secondary metabolites (31%), energy (9%) and xenobiotics (6%). Especially, the pathways of the immune system included the T cell receptor signaling pathway and biotin metabolism pathway. In addition, phosphatidylinositol signaling system and glycosylphosphatidylinositol (GPI)-anchor biosynthesis were also identified in our study.

**Characteristics of the differentially expressed proteins.** There were 2670 differentially expressed (DE) proteins (Supplementary Table S4) out of the 10367 proteins (Supplementary Table S3) between the treatment and control samples. The comparison design is displayed as Fig. 3C, WT treated with TA (WT + TA) is the control group for all treated group including WT group. WT vs WT + TA represented proteome changes in WT upon toxin treatment; JA and TA treated WT (WT + TA + JA) vs WT + TA represented JA induced proteome

Classification <sup>a</sup>	KEGG pathways	Sequence number <sup>b</sup>
Nucleotide	Purine metabolism	262
	Pyrimidine metabolism	93
	Amino sugar and nucleotide sugar metabolism	93
	Pentose and glucuronate interconversions	74
	Pentose phosphate pathway	68
	Phenylalanine metabolism	147
Amino acid	Glutathione metabolism	87
	Arginine and proline metabolism	77
	Glycine, serine and threonine metabolism	77
	Cysteine and methionine metabolism	71
	Tryptophan metabolism	68
	Valine, leucine and isoleucine degradation	63
	Aminobenzoate degradation	58
	Aminoacyl-tRNA biosynthesis	54
	Tyrosine metabolism	52
	Alanine, aspartate and glutamate metabolism	51
	Lysine degradation	46
	Cyanoamino acid metabolism	46
	$\beta$ -Alanine metabolism	44
	Phenylalanine, tyrosine and tryptophan biosynthesis	40
Carbohydrate	Starch and sucrose metabolism	212
	Galactose metabolism	82
Lipid	Glycerolipid metabolism	85
	Phosphatidylinositol signaling system	70
	Fatty acid degradation	68
	Inositol phosphate metabolism	59
	$\alpha$ -Linoleic acid metabolism	54
	Glycerophospholipid metabolism	48
	Fatty acid biosynthesis	42
	Biosynthesis of unsaturated fatty acids	41
Secondary metabolites	Pyruvate metabolism	93
	Thiamine metabolism	80
	Glyoxylate and dicarboxylate metabolism	73
	Methane metabolism	71
	Flavonoid biosynthesis	49
	Porphyrin and chlorophyll metabolism	45
	Ascorbate and aldarate metabolism	43
Energy	Glycolysis/ Gluconeogenesis	118
	Carbon fixation in photosynthetic organisms	87
	Fructose and mannose metabolism	64
	Oxidative phosphorylation	58
	Carbon fixation pathways in prokaryotes	57
	Citrate cycle (TCA cycle)	48
Xenobiotics	Drug metabolism - cytochrome P450	70
	T cell receptor signaling pathway	66
	Metabolism of xenobiotics by cytochrome P450	65
	Drug metabolism - other enzymes	45

**Table 1. The most enriched Kyoto Encyclopaedia of Genes and Genomes (KEGG) pathways.** <sup>a</sup>KEGG pathways were classified by metabolic pathways of different molecules. <sup>b</sup>Sequence number involved in the corresponding KEGG pathways above 40 were presented.

changes upon TA treatment; *jai1* treated with TA (*jai1* + TA) vs WT + TA showed the COI1-dependent proteome changes during the response of plant to TA. 2400 out of 10367 proteins were excluded from the quantitative analysis because variations were detected within biological replicates within each treatment (Supplementary Figure S2).

Among the DE proteins, there were 921, 819, 1576 proteins in WT vs WT+TA, WT + TA + JA vs WT + TA, and *jai1* + TA vs WT + TA, respectively (Fig. 3C). It indicates that the COI1 mutation can give rise to the largest

Related Pathway	Sequence Id <sup>a</sup>	Protein name	WT+TA+JA/ WT+TA <sup>b</sup> Average fold change <sup>c</sup>	WT+TA+JA/ WT+TA <i>p</i> -value <sup>d</sup>
Cell death	Solyc11g022590.1.1_1	Kunitz-like protease partial	29.9158	0.0007
	Solyc04g080960.2.1_1	Cysteine proteinase rd19a-like	2.0656	0.0055
	Solyc00g071180.2.1_1	Cysteine protease inhibitor	23.6525	0.0140
	Solyc03g097270.2.1_1	Cysteine proteinase inhibitor	6.6684	0.0010
	Solyc12g011140.1.1_1	Subtilisin-like protease	4.6594	0.0003
	Solyc02g092670.1.1_1	Subtilisin-like protease-like	2.5589	0.0059
Cell death	Solyc08g079900.1.1_1	Subtilisin-like protease-like	1.7299	0.0001
	Solyc08g079870.1.1_1	Subtilisin-like protease-like	3.5601	0.0059
	Solyc04g076190.1.1_1	Aspartic proteinase nepenthesin-1-like	12.9902	0.0173
Jasmonate	Solyc01g008620.2.1_1	3- $\beta$ -glucan endohydrolase short	5.4506	0.0220
	Solyc03g116110.2.1_1	$\alpha$ $\beta$ -hydrolases superfamily protein	6.5446	0.0269
Ethylene	Solyc01g008330.2.1_1	Biotin carboxylase chloroplastic-like	4.6059	0.0258
	Solyc11g013170.1.1_1	Probable n-succinyl-diaminopimelate Aminotransferase-like	3.0551	0.0392
Abscisic acid	Solyc01g097520.2.1_1	Annexin d4-like	1.7482	0.0007
	Solyc02g081170.2.1_1	Plastid-lipid-associated chloroplastic-like	3.4850	0.0124
	Solyc09g082780.2.1_1	Stem-specific protein TSJT1-like	7.6080	0.0212
	Solyc05g009600.2.1_1	PP2A 65 kda regulatory subunit a beta isoform-like	1.9054	0.0118
Resistance	Solyc02g082920.2.1_1	Class II chitinase	8.8545	0.0148
	Solyc10g055810.1.1_1	Class I chitinase	0.7325	0.0078
	Solyc05g007610.2.1_1	Late blight resistance identical	5.9576	0.0179
	Solyc01g090430.2.1_1	Late blight resistance protein homolog r1a-10-like	2.1669	0.0238
	Solyc09g011590.2.1_1	Probable glutathione s-transferase-like	2.0707	0.0002
	Solyc09g090330.2.1_1	Harpin binding protein 1	2.6641	0.0277
	Solyc09g090980.2.1_1	Pathogenesis-related protein 10	14.2910	0.0001
	Solyc09g090990.2.1_1	Pathogenesis-related protein 10	83.1215	0.0356
	Solyc09g091000.2.1_1	Pathogenesis-related protein sth-2-like	0.4453	0.0131
DNA repair	Solyc08g074290.2.1_1	DNA repair ATPase-related family protein	1.6077	0.0058
	Solyc02g021650.2.1_1	DNA damage-binding protein 1-like	3.2392	0.0350
	Solyc02g082660.2.1_1	DNA mismatch repair protein	8.3748	0.0406

**Table 2. Interesting and novel proteins changed by JA treatment in the process of TA induced PCD.**

<sup>a</sup>Accession numbers from GenBank database or Sol Genomics Network (SGN). <sup>b</sup>(WT + TA + JA/WT + TA) represented JA and TA treated WT vs TA treated WT. <sup>c</sup>Red color represents that the protein was up-regulated, green color represents that the protein was down-regulated. <sup>d</sup>*t*-test indicates significant difference in expression of these proteins between WT treated with JA and TA and WT treated with TA alone, with *p*-value threshold values ( $\alpha = 0.05$ ).

changes to tomato proteome. Interestingly, most DE proteins in WT after TA treatment or TA + JA treatment showed higher number of increasing patterns, while those in *jail* after TA treatment exhibited similar number of increasing and decreasing patterns compared with WT. The expression patterns of the differentially expressed proteins in each comparison groups were clustered and displayed as a heat map in Supplementary Figure S5. Among the increased proteins, 61 were shared by the three comparisons, whereas only one protein was found

Related pathway	Sequence Id <sup>a</sup>	Protein name	<i>jaiI</i> +TA/ WT+TA <sup>b</sup> AVE Fold Change <sup>c</sup>	<i>jaiI</i> +TA/ WT+TA <i>p</i> -value <sup>d</sup>
<b>Redox</b>	Solyc04g025650.2.1_1	Monooxygenase 1	0.3778	0.0099
	Solyc08g069040.2.1_1	Peroxidase 51-like	4.0760	0.0333
	Solyc12g056250.1.1_1	Glutathione s-transferase t1-like	4.2429	0.0226
	Solyc01g007740.2.1_1	2-cys peroxiredoxin bas1- chloroplastic-like	9.1890	0.0152
	Solyc07g056500.2.1_1	Probable glutathione s-transferase	10.1470	0.0024
	Solyc02g086090.2.1_1	Mannose-6-phosphate isomerase 1-like	25.8542	0.0083
<b>Ceramide metabolic process</b>	Solyc02g078180.2.1_1	Uncharacterized loc101209711	0.0350	0.0001
	Solyc05g013720.2.1_1	Melibiose family protein	3.9386	0.0001
	Solyc03g098220.2.1_1	Serine palmitoyltransferase	1.4553	0.0020
<b>Autophagy</b>	Solyc07g005970.2.1_1	Autophagy-related protein 11	0.4675	0.0001
	Solyc09g020110.2.1_1	Ribonuclease 2-like	8.4530	0.0493
<b>Cell death</b>	Solyc03g098790.1.1_1	Kunitz-type protease inhibitor precursor	2.0055	0.0196
	Solyc00g130800.1.1_1	Peptidase c14 caspase catalytic subunit p20	1.6202	0.0377
	Solyc09g098150.2.1_1	Metacaspase type II	1.3907	0.0212
<b>JA synthesis</b>	Solyc07g007870.2.1_1	12-oxophytodienoate reductase 3	4.3415	0.0441
	Solyc11g069800.1.1_1	Allene oxide synthase	9.4840	0.0030
<b>JA response</b>	Solyc01g010950.2.1_1	Dual specificity protein kinase spla-like	0.4950	0.0182
	Solyc05g053170.2.1_1	Chalcone synthase	0.6337	0.0011
	Solyc05g050590.2.1_1	Phosphoinositide 4-kinase gamma 4	0.4500	0.0001
	Solyc04g079720.2.1_1	3-n-debenzoyl-2-deoxytaxol n- Benzoyltransferase-like	0.3109	0.0002
	Solyc02g093790.2.1_1	Probable carboxylesterase 11-like	0.1006	0.0030
<b>ET synthesis</b>	Solyc03g116110.2.1_1	1-aminocyclopropane-1-carboxylate oxidase Homolog 1-like	0.4762	0.0189
<b>ET response</b>	Solyc04g009850.2.1_1	Response regulator 1	0.1719	0.0051
	Solyc04g051080.1.1_1	Ethylene-responsive transcription factor rap2-7-like	0.3854	0.0148
	Solyc10g084340.1.1_1	AP2-like ethylene-responsive transcription factor ail5-like	4.9193	0.0292
	Solyc07g018290.2.1_1	Ein3-binding F-box protein 1-like	5.4162	0.0249
<b>SA related</b>	Solyc12g009560.1.1_1	Acyl-protein thioesterase 1-like	5.0404	0.0297
	Solyc11g012070.1.1_1	Shikimate kinase like 1	5.4686	0.0014
	Solyc02g094420.2.1_1	Peptidyl-prolyl cis-trans isomerase Chloroplastic-like	2.7358	0.0206
	Solyc02g086910.2.1_1	Cytochrome b6-f complex iron-sulfur chloroplastic-like	2.3017	0.0248
	Solyc12g005630.1.1_1	Leucine-rich repeat receptor-like tyrosine-protein kinase at2g41820-like	3.4704	0.0222
	<b>ABA response</b>	Solyc11g017270.1.1_1	Cbl-interacting serine threonine-protein kinase 3-like	14.076
Solyc05g009600.2.1_1		PP2A 65 kda regulatory subunit a $\beta$ isoform-like	2.3164	0.0206
Solyc09g082780.2.1_1		Stem-specific protein tsjt1-like	7.5958	0.0002
Solyc10g055800.1.1_1		Class I chitinase	4.2751	0.0024
<b>Receptor like Kinase</b>		Solyc02g014320.1.1_1	Probable receptor-like protein kinase at5g47070-like	0.4852
	Solyc07g066550.2.1_1	Probable LRR receptor-like serine threonine-protein kinase at1g56130-like	3.0263	0.0001
	Solyc03g019980.1.1_1	Probable LRR receptor-like serine threonine-protein kinase at3g47570-like	2.1233	0.0012

**Table 3. COI1-dependent pathways in response to TA.** <sup>a</sup>Accession numbers from GenBank database or Sol Genomics Network (SGN). <sup>b</sup>(*jaiI* + TA/WT + TA) represented *jaiI* treated with TA vs WT treated with TA. <sup>c</sup>Red color represents that the protein was up-regulated, green color represents that the protein was down-regulated. <sup>d</sup>*t*-test indicates significant difference in expression of these proteins between *jaiI* treated with TA and WT treated with TA, with *p*-value threshold values ( $\alpha = 0.05$ ).

to be decreased in all the comparisons (Fig. 3C), each comparison group also contained their own DE proteins. These proteins present a global view of WT and *jai1* proteome level responses to TA and JA treatment. The expression patterns across each contrasts were classified into 24 categories, as was shown in Supplementary Table S1.

The biological process classification of the 10367 proteins was used as the reference for the functional analysis of DE proteins. We have presented the comparison of functional classification between the 10367 overall detected and 2670 differentially expressed proteins in Supplementary Figure S3, and we found that the biological function processes of the 2670 DE proteins distributed similarly with the overall identified proteins.

**JA-regulated proteins in TA induced PCD process.** As shown by the previous physiological results that JA promoted PCD, we further investigated JA-regulated proteins in TA induced PCD process, by checking the DE proteins in WT + TA + JA vs WT + TA comparison. The DE proteins related to cell death, JA, ET, ABA, DNA repair and resistance were listed in Table 2. In animal systems, cysteinyl aspartate-specific proteinases (caspases), serine proteases and specific protease inhibitors play crucial roles during the regulation of PCD process<sup>24</sup>. We found that several proteases were increased by JA treatment, including a kunitz-like protease partial, a cysteine proteinase RD19a-like, an aspartic proteinase nepenthesin-1-like and a  $\beta$ -1, 3-glucanase. Previous study showed that some caspase-like activities are attributable to plant subtilisin-like proteases (SBTs), which are related to cell death<sup>25</sup>. We detected four SBT or SBT like proteins in tomato leaves which were increased by JA treatment. Furthermore, cysteine protease inhibitor (CPI) is known as one of the specific inhibitors of PCD in plant cells<sup>26</sup>. In our experiment, CPI was increased by 23 fold in the WT leaves after treatment with JA and TA together, while increased by two fold after singly TA treatment. These results indicated that TA treatment also induces the expression of some PCD suppressors, which could be enhanced by JA treatment. In addition, two JA response proteins,  $\alpha\beta$ -hydrolases superfamily protein and biotin carboxylase chloroplastic-like, were found to be involved in TA induced PCD. An ET synthesis related protein, probable N-succinyl diaminopimelate aminotransferase-like, was up-regulated by TA + JA treatment compared with TA treatment alone. Four abscisic acid (ABA) response proteins (annexin D4-like, plastid-lipid-associated chloroplastic-like, stem-specific protein TSJT1-like, and PP2A 65 kda regulatory subunit  $\alpha\beta$  isoform-like) were also increased by JA treatment in response to TA, indicating the possible involvement of ET and ABA pathway in TA induced PCD.

Pathogenesis-related proteins (PRs) are general markers for basal defense response. Two PR10 proteins increased significantly after TA + JA treatment compared with TA treatment alone, while PR-sth2-like protein and PR1 were decreased by JA treatment. Besides, several late blight resistance proteins, a chitinase and a harpin binding protein were also increased by TA + JA treatment, implying that JA could promote the synthesis of resistance proteins. The DNA damage response (DDR) plays an important role against detrimental effects of stress<sup>27</sup>. Three DNA repair related proteins (DNA repair ATPase-related family protein, DNA damage-binding protein 1-like, and DNA mismatch repair protein), were increased by JA during TA induced PCD.

**COI1-dependent signaling pathways in response to TA.** We were interested in COI1-dependent signaling pathways in response to TA, as previous results have shown that COI1 impairment inhibits TA induced PCD in tomato leaves. DE proteins between TA treated *jai1* and WT were classified as COI1-dependent proteins in response to TA. The candidate proteins related to defense response and programmed cell death were listed in Table 3. Firstly, six reductase proteins (peroxidase 51-like, glutathione s-transferase T1-like, 2-cys peroxidase, BAS1-chloroplastic-like, probable glutathione s-transferase, mannose- 6-phosphate isomerase 1-like) were significantly higher in *jai1*, whereas an oxidase protein (monooxygenase 1) was decreased in *jai1* compared to WT after TA treatment, suggesting that ROS may act downstream of COI1 to promote TA induced PCD process.

The levels of two ceramide synthesis related proteins, melibiase family protein and serine palmitoyltransferase, were higher in *jai1* than in WT after TA treatment, indicating that COI1-dependent JA signaling might promote TA induced PCD by regulating the biosynthesis of ceramide. Proteins related to autophagy, which plays a role in maintaining the intracellular homeostasis, were also found among the list of DE proteins. Autophagy-related protein 11 (ATG 11) was decreased in *jai1*, whereas RIBONUCLEASE 2-LIKE as a negative regulator of autophagy, was increased in *jai1* after TA treatment. The results indicated that autophagy might be promoted by COI1-dependent JA signaling, and related to inhibition of TA induced PCD. Kunitz Trypsin Inhibitor (KTI1) was previously proved to be an antagonist of cell death triggered by phytopathogens and Fumonisin B1 in *Arabidopsis*<sup>28</sup>. In the current survey, it was increased in *jai1* by two folds. Metacaspase type II and the peptidase C14 caspase catalytic subunit P20, as potential PCD regulators, were increased slightly in *jai1*. This result was different from the former report that the type-II metacaspase from tomato (LemCA1) was not increased during chemical induced PCD in suspension-cultured tomato cells<sup>29</sup>. As tomato genome contains at least two type-II metacaspases, we speculate that different metacaspases might have distinct functions during PCD process, and display different expression patterns. Most of the above results partly explained why PCD was lighter in *jai1* than in WT.

Our previous studies have shown that JA, ET and SA are involved in the response of tomato leaves to AAL or AAL toxin<sup>30</sup>. In the current survey, we paid more attention to the proteins relevant to these three hormone pathways. The expression of two JA biosynthetic genes, 12-oxophytodienoate reductase 3 and allene oxide synthase were increased in *jai1*, while some of the JA response genes were decreased, due to the impaired perception of JA. ET biosynthesis and response were inhibited, whereas SA synthesis and response were enhanced in *jai1* mutant, suggesting that COI1-dependent JA signaling acts synergistically with ET, and antagonistically with SA during response to TA. Several proteins in ABA response pathway, were decreased in *jai1* after TA treatment (Table 3), indicating that COI1-dependent JA signaling might interact with ABA pathway in regulating TA induced PCD.



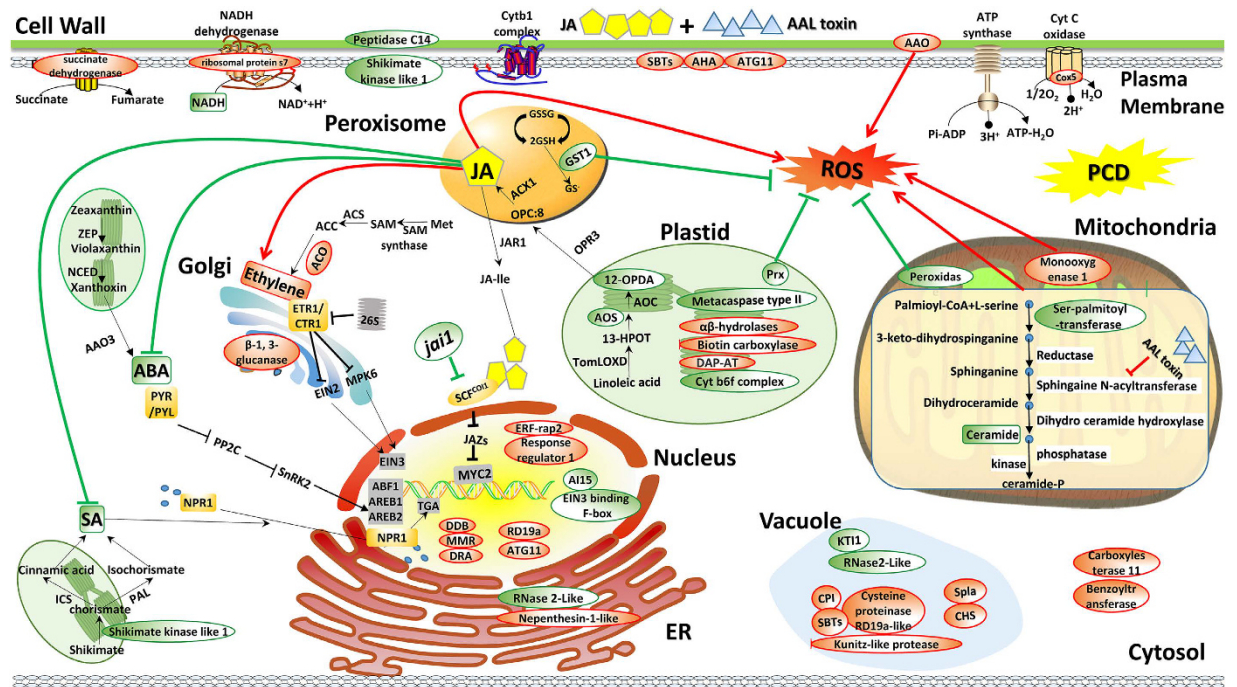


**Figure 4.** A putative model showing possible mechanisms of JA regulated AAL toxin response in *Solanum Lycopersicum*. The DE proteins caused by JA treatment and COI1 mutation during AAL toxin induced PCD were used to construct the model, and the impairment of COI1 induced protein changes were presented with the contrary change patterns. The identified proteins were assigned to different organelles or groups according to their subcellular localization and molecular functions. Up-regulated proteins are highlighted red and down-regulated proteins are colored green. Arrows and bars represent positive and negative regulation respectively. Red solid lines indicate that the pathways are up-regulated or promoted by JA during TA response, green solid lines with bars or arrows indicate that the pathways are down-regulated by JA during TA response, black solid lines with arrows links the proteins within the same pathway. TA induce PCD by inhibiting the synthesis of ceramide and inducing the overproduction of ROS, COI1-dependent JA pathway may promote this PCD progress by influencing the ROS production and scavenging, other hormone signaling pathways or some possible PCD regulators such as caspase-like proteins, autophagy and DNA repair related proteins. AAO, L-ascorbic acid oxidase; ABI1, ABA insensitive1; ACO1, 1-aminocyclopropane-1-carboxylate oxidase homolog 1-like; AHA, plasma membrane H<sup>+</sup>-ATPase; AOS, allene oxide synthase; ATG11, autophagy related protein 11; CHS, chalcone synthase; CPI, cysteine protease inhibitor; Cyt, Cytochrome; DAP-AT, probable n-succinyldiaminopimelate aminotransferase-like; DDB, DNA damage binding proteins; DDR, DNA damage response; DRA, DNA repair ATPase-related family protein; ER, endoplasmic reticulum; GST, glutathione S-transferase; Golgi, golgi complex; KTI1, kunitz trypsin inhibitor; MMR, DNA mismatch repair; NAT, nucleobase-ascorbate transporter 6-like; Prx, Peroxiredoxin; RNase E, Ribonuclease 2-Like; SBTs, subtilisin-like proteases; TF, transcription factor.

## Discussion

Previous studies have shown that AAL toxin can inhibit ceramide biosynthetic enzymes and lead to PCD in sensitive *asc/asc* tomato species, due to the reduced sphingolipids and accumulated dihydrospingosine (DHS) and 3-ketodihydrospingosine (3-KDHS)<sup>31,32</sup>. However, the underlying mechanism from toxin perception to PCD process is poorly understood in plants. Our research explored the potential pathways and regulators in AAL toxin induced PCD and the role of COI1-dependent JA signaling pathway in regulating the PCD process.

Proteases specifically the classical proteolytic enzymes called caspases, were reported to be participated in the regulation of animal PCD, implies that proteases may be involved in regulation of plant PCD<sup>33</sup>. Several reports also have proved the involvement of proteases in regulating plant PCD. Both protease activity and cell death were inhibited by soybean trypsin inhibitor, while exogenous application of another serine protease prematurely triggered cell death<sup>34</sup>. In tobacco, inhibition of the induced cysteine protease activity by ectopic expression of a cysteine protease inhibitor (CPI) gene, blocked the PCD triggered either by an avirulent pathogen or by ROS<sup>26</sup>. We identified several JA treatment induced proteases during AAL toxin induced PCD, including a kunitz-like protease, a cysteine proteinase RD19a-like, an aspartic proteinase nepenthesin-1-like, a β-1, 3-glucanase and four SBT like proteins (Table 2). Moreover, we also found that CPI was increased by two fold after toxin treatment alone, while it was increased by 23 fold after TA and JA treatment. The results suggest that TA treatment promoted the expression of some specific proteases to induce PCD, and JA treatment enhanced the response. However, two other caspase-like proteases, metacaspase type II and the peptidase C14 caspase catalytic subunit P20, were increased slightly in *jai1* and decreased in WT after TA treatment, suggesting that these two proteases

may function as negative regulators of plant PCD. Kunitz trypsin inhibitor gene (KTI1) was proved to play a regulatory role in PCD antagonizing pathogen and Fumonisin B1 induced cell death<sup>28</sup>. The KTI1 found in our study was increased in *jai1* by two folds in comparison with WT after TA treatment (Table 3), implying that KTI1 is also a negative regulator of plant PCD induced by TA.

Mitochondrial quality control is important in maintaining proper cellular homeostasis, and selective mitochondrial degradation by autophagy (mitophagy) is suggested to play an important role in quality control<sup>34</sup>. Selective autophagy includes the cytoplasm to vacuole targeting (Cvt) pathway<sup>35</sup> and pexophagy<sup>36</sup>. To date, 31 autophagy-related genes have been identified, which function as the molecular machinery for autophagy. Among them, ATG 11 is essential for mitophagy, acting as an adaptor protein that is needed along with ATG 19 to recruit the Cvt complex to phagophore assembly site (PAS), where the sequestering cytosolic vesicles are generated<sup>37</sup>. In the present study, ATG 11 in tomato was found to be decreased by COI1 impairment after AAL toxin treatment. Conversely, the autophagy negative regulator RIBONUCLEASE 2-LIKE was significantly increased by COI1 impairment during AAL toxin induced PCD, suggesting that autophagy in *jai1* was suppressed, leading to reduced cell death.

In addition to the putative PCD regulators conserved throughout animal and plant, there also exist some plant-specific mediators of PCD. Various plant hormones are strong candidates, and supporting evidence began to accumulate<sup>38</sup>. Our previous studies showed that COI1-dependent JA pathway acts upstream of ET to promote TA-triggered PCD<sup>11</sup>, which was further verified by the proteomic evidence in this study. The modulator of AAL cell death 1 (MACD1), which is an AP2/ERF transcription factor acting downstream of ET signaling, has been reported to positively regulate AAL triggered cell death<sup>29</sup>. We found that an AP2/ERF transcription factor RAP2-7-like was decreased significantly in *jai1* during response to TA, suggesting that COI1-mediated JA signaling promote TA induced PCD by enhancement of ET response via RAP2-7 like. The resistance of tomato plants to AAL and AAL toxin is enhanced by SA pathway<sup>30</sup>. The proteins related to SA biosynthesis and response were increased in *jai1* mutant after TA treatment, indicating that COI1-dependent JA pathway interacts with SA pathway in an antagonistic way to enhance TA induced PCD.

ROS have emerged as important signals in activation of plant PCD. Studies on exogenous application of H<sub>2</sub>O<sub>2</sub> confirmed the role of H<sub>2</sub>O<sub>2</sub> as a cell death trigger<sup>39</sup>. Zhang<sup>40</sup> also proved that AAL toxin induced PCD is closely related to the production of ROS. In the present study, the decreased levels of H<sub>2</sub>O<sub>2</sub> and O<sub>2</sub><sup>-</sup> in *jai1* is consistent with the reduced cell death in *jai1* after AAL toxin treatment, suggesting that JA exert its effects on plant PCD through regulation of ROS accumulation. Inhibitors of ET biosynthesis or perception blocked H<sub>2</sub>O<sub>2</sub> production and cell death in tomato suspension cells<sup>41</sup>, therefore the decreased ROS production in *jai1* might be owing to the inhibited ET pathway. In addition, JA also acted through regulation of ET pathway in many cases, for example, JA-promoted lycopene was correlated with JA-stimulated ET production<sup>42</sup>, and both ET biosynthesis and the signaling pathway are strongly decreased in *jai1* leaves inoculated with AAL when compared with WT<sup>30</sup>. The *Arabidopsis* jasmonate-insensitive mutant *jar1* shows enhanced cell death after exposure to O<sup>3-</sup>, and wounding or treatment with JA has been shown to reduce O<sup>3-</sup> induced cell death and ROS levels<sup>16</sup>, in contrast to our finding in TA induced PCD. Complex mechanisms exist among PCD processes induced by distinct factors, which may be species-specific. Besides JA and ET, ABA seems to act downstream of COI1-mediated JA signaling in promoting TA induced PCD. Virus induced gene silencing (VIGS) analyses proved that AAL toxin triggered cell death is dependent on the mitogen-activated protein kinase MEK2 in tobacco<sup>43</sup>. We observed that the mitogen-activated protein kinase 9-like (MAPK9-Like) was significantly decreased in *jai1* after TA treatment, suggesting a possible role of MAPK9-Like in response to TA in tomato leaves.

The CCR4-NOT transcription complex has been well known as mRNA deadenylases in eukaryotic cells. Liang *et al.*<sup>44</sup> proved that the homologs of CCR4-associated factor 1 (CAF1) in *Arabidopsis* are involved in defence responses to pathogen infections. In our results, two subunits of CCR4-NOT transcription complex were upregulated in *jai1* mutant compared with the wild type (Supplementary Table S4), indicating that the CCR4-NOT transcription complex is also involved in the defence responses to AAL toxin in tomato.

In plants, plasma membrane (PM) H<sup>+</sup>-ATPases are the primary pumps responsible for the establishment of cellular membrane potential, which are absolutely essential for normal plant growth and development<sup>45</sup>. A PM H<sup>+</sup>-ATPase was slightly decreased by TA treatment, suggesting its function in toxin response. Moreover, if DNA damage is left unrepaired or mis-repaired, it can be changed into a mutation. Three DNA damage response related proteins were found to be increased by JA, indicating that JA promotes the DNA repair process to cope with the occurrence of the PCD and mutation.

In summary, we explored the mechanisms in JA regulation of AAL toxin induced PCD using comparative proteomics. We identified a large number of DE proteins induced by TA + JA treatment in WT and *jai1*. The DE proteins revealed by iTRAQ quantitative proteomics approach in this study help to elucidate the molecular regulating network of COI1-dependent JA pathway in PCD. Numerous new components in cell death machinery were identified, which were summarized in several pathways and represented in Fig. 4. TA causes PCD by inhibiting the synthesis of ceramide and inducing the overproduction of ROS. COI1-dependent JA pathway may promote this PCD progress by influencing the ROS production and scavenging, other hormone signaling pathways or some possible PCD regulators such as caspase-like proteins, autophagy and DNA repair related proteins. Our findings have deepened the understanding of the mechanisms in fungal toxin induced PCD and JA mediated plant defense in response to the fungal toxin. Many of the proteins identified in the present study including their modifications are interesting targets for further genetic and molecular studies to establish the precise roles in cell death and defense regulatory networks.

## Methods

**Plant growth and selection of *jai1* homozygotes.** Tomato (*S. lycopersicum*) cultivar Castlemart (CA) is the parental line for JA insensitive mutant *jai1*. Seeds were germinated on the filter paper after

treatment with 1% sodium hypochlorite (NaOCl) for 10 minutes. The germinated seedlings were treated with 1 mM MeJA (Sigma, St Louis, MO, USA). Approximately 24 h or 36 h later, MeJA-insensitive seedlings (roots growth is not inhibited by MeJA) were selected by PCR using genomic DNA using three primers below: P1: 5'-GTGGAGACGATATGTTGAGACTAA-3'; P2: 5'-CCATGGAG TCCATCACCTAACAGT-3'; P3: 5'-GTGGTCAGATCAGAGCCCCTATT-3'; PCR product with only a 777 bp band are homozygous *jai1* mutant. Seedlings were grown in the growth chamber with day/night temperature of 26/18 °C (16/8h). All experiments were carried out using fully expanded leaflets from nodes 4–6 (except for the terminal leaflets) of 7-week-old tomato plants. *jai1* homozygotes were screened according to Li *et al.*<sup>14</sup>.

**Detached leaflet treatment with JA and AAL Toxin.** Treatment was performed as described earlier<sup>46,47</sup>. The treatment solutions contained different concentrations of JA (0, 10, 100, or 500  $\mu$ M) and 0.2  $\mu$ M TA (the most common kind of AAL toxin<sup>8</sup>) under continuous light at 25 °C, sodium phosphate buffer (SPB, pH 7.0) was used as a control. Four excised leaflets from individual plants were incubated for different time periods on a piece of filter paper in one Petri dish.

**Cell death assays.** Cell death was detected using trypan blue staining. Detached leaves were submerged in the farmers solution (acetic acid:ethanol:chloroform = 1:6:3, V/V/V) to make it transparent, dyed in the solution involving 0.05% w/v trypan blue and ethanol (1:2 V/V), and then washed with water and decolorized in saturated chloral hydrate.

**Detection of malondialdehyde content.** Leaf samples (0.4 g each) were ground in 4 mL of phosphate buffer (0.05 M PBS, pH 7.8, 0.2 mM EDTA, 2% polyvinyl pyrrolidone), centrifuged at 12000 g for 20 min and the total supernatant was used for the measurement. The measurement of malondialdehyde (MDA) content was calculated from the thiobarbituric acid (TBA) reaction using an extinction coefficient of 155  $\text{mM}^{-1} \text{cm}^{-1}$ <sup>48</sup>. One milliliter supernatant was added into 3 mL of TBA solution, kept at 95 °C for 30 min, centrifuged at 1500 g for 10 min, and then MDA content was calculated according to the absorbance measured at 600 nm, 532 nm, and 450 nm, respectively.

**Detection and quantification of H<sub>2</sub>O<sub>2</sub> and superoxide.** Intracellular H<sub>2</sub>O<sub>2</sub> was detected by 3, 3'-diaminobenzidine tetrahydrochloride (DAB) staining, showing a brown stain caused by the polymerization of DAB<sup>21</sup>. Superoxide (O<sub>2</sub><sup>-</sup>) was detected by staining leaves with nitro blue tetrazolium chloride (NBT), which is reduced by superoxide to form a dark blue, water-insoluble formazan<sup>22</sup>. The O<sub>2</sub><sup>-</sup> production rate was measured by analyzing the nitrite formation from hydroxylamine in the presence of O<sub>2</sub><sup>-</sup>. Frozen leaf segment was homogenized with 3 mL of 65 mM Phosphate Buffered Saline (PBS, pH 7.8) and centrifuged at 5000 g for 10 min. After incubation in the solution containing 0.9 mL of 65 mM PBS (pH 7.8), 0.1 mL of 10 mM hydroxylamine hydrochloride, and 1 mL of the supernatant at 25 °C for 20 min, 17 mM sulphanimide and 7 mM anaphthylamine were added. Ethylether in the same volume was added and centrifuged at 1500 g for 5 min. The absorbance in the aqueous solution was monitored at 530 nm<sup>49</sup>. Quantification of H<sub>2</sub>O<sub>2</sub> was done as follows: 0.4 g samples were ground in cold acetone and centrifuged at 3000 g for 10 min, the supernatant was then mixed with 0.2 mL of 20% TiCl<sub>4</sub> and 0.4 mL of ammoni, the precipitation was washed with acetone for five times, finally dissolved in 3 mL of 2 M H<sub>2</sub>SO<sub>4</sub>, and determined spectra-photometrically by measuring the absorbance at 595 nm.

**Protein extraction and quantification.** Proteins from tomato leaves of four biological replicates were prepared according to Hurkman and Tanaka<sup>50</sup> with the following modifications. Samples were ground in liquid nitrogen into fine powder and incubated in extraction buffer (0.1 M Tris-HCl pH 8.8, 10 mM EDTA, 0.2 M DL-Dithiothreitol, 0.9 M sucrose), continued by grinding in a fume hood, and then the extract was agitated for 2 hrs at room temp. After washing twice with 0.1 M ammonium acetate in methanol and twice with 80% acetone, the dried pellet was dissolved with 2D buffer (8 M Urea, 4% CHAPS, 40 mM Tris-base, 2 M Thiourea). Protein assays were performed using an EZQ Protein Quantitation Kit (Invitrogen, Carlsbad, CA, USA) with the SoftMax Pro Software v5.3 (Molecular Devices, Downingtown, PA, USA).

**Protein precipitation, iTRAQ labeling, strong cation exchange, LC-MS/MS.** For each sample, 50  $\mu$ g protein was dissolved in the dissolution buffer with 1  $\mu$ l of denaturant in the iTRAQ reagents 8-plex kit (AB Sciex, Inc., Foster City, CA, USA). The samples were reduced with Tris (2-Carboxyethyl) Phosphine (TCEP), alkylated with methyl methanethiosulfonate (MMTS), trypsin-digested, and labeled according to the manufacturer's instructions for the iTRAQ reagents 8-plex kit (AB Sciex Inc., California, USA). Mock lines (wild type, CA) were labeled with iTRAQ tags 113 and 117; TA treated WT lines were labeled with tags 114 and 118; TA and jasmonic acid treated WT lines were labeled with tags 115 and 119; TA treated *jai1* lines were labeled with tags 116 and 121. The biological quadruplicates were analyzed to account for variation among individuals. The combined peptide mixtures were desalted and lyophilized. After labeling, samples were combined, desalted with solid phase extraction (The Nest Group, Inc., Southborough, MA, USA), lyophilized and dissolved in strong cation exchange (SCX) solvent A (25% (v/v) acetonitrile, 10 mM ammonium formate and 0.1% (v/v) formic acid (pH 2.8)). The peptides were fractionated using an Agilent HPLC system 1260 with a polysulfoethyl column (2.1 mm  $\times$  100 mm, 5  $\mu$ L, 300 Å; PolyLC, Columbia, MD, USA), flow rate of 0.2 mL/min. Peptides were eluted with a linear gradient of 0–20% solvent B (25% (v/v) acetonitrile and 500 mM ammonium formate (pH 6.8)) over 50 min, followed by ramping up to 100% solvent B in 5 min. The absorbance at 280 nm was monitored; 12 fractions were collected and lyophilized. The fractions were resuspended in LC solvent A (0.1% formic acid in 97% water, 3% acetonitrile). A hybrid quadrupole Orbitrap (Q Exactive) MS system (Thermo Fisher Scientific, Bremen, Germany) was used with high energy collisional dissociation (HCD) after each MS. The instrument was run in data dependent mode

with a full MS (400–2000 m/z) resolution of 70,000 and five ms/ms (17500 resolution, HCD NCE = 28%, isolation width = 3 Th, first mass = 105 Th., 5% underfill ratio, peptide match set to 'preferred', and an AGC target of  $1e^6$ ). Dynamic exclusion of 10 s was applied to prevent repeated analyses of the same peptides, and a lock mass of m/z 445.12003 (polysiloxane ion) was used for real-time internal calibration. The MS system was interfaced with an automated Easy-nLC 1000 system (Thermo Fisher Scientific, Germering, Germany). Each sample fraction was loaded on an Acclaim Pepmap 100 pre-column (20 cm × 75 μm; 3 μm-C18) and separated using a PepMap RSLC analytical column (250 cm × 75 μm; 2 μm-C18) with a flow rate at 350 nl/min. A linear gradient of solvent A (0.1% formic acid) to solvent B (0.1% formic acid, 99.9% acetonitrile) was run for 95 min, followed by a ramp to 98% B for 5 min. The MS proteomics data have been deposited in the ProteomeXchange Consortium<sup>51</sup> via the PRIDE partner repository with the data set identifier PXD002864 and 10.6019/PXD002864.

**iTRAQ LC-MS/MS data analysis.** The raw MS/MS data files were searched against the specified non-redundant database (combined Uniprot, <http://www.uniprot.org/uniprot/?query=solanum+lycopersicum&sort=score>; NCBI, <http://www.ncbi.nlm.nih.gov/gquery/?term=solanum+lycopersicum>; Phytosome, <http://www.phytosome.net/tomato.php>) using the Fraglet and Taglet searches under the Paragon™ algorithm<sup>52</sup> of ProteinPilot v.4.5 software (AB Sciex, Inc.). Plant species, fixed modification of methylmethane thiosulfate-labeled cysteine, fixed iTRAQ modification of amine groups in the N-terminus and lysine, and variable iTRAQ modifications of tyrosine were considered. In addition, the iTRAQ data were analyzed using Proteome Discoverer v1.4 (Thermo Fisher Scientific, Bremen, Germany) and the following parameters: peptide tolerance at 10 ppm, tandem MS tolerance at ±0.01 Da, peptide charges of 2+ to 5+, trypsin as the enzyme, allowing one missed cleavage, iTRAQ label and methyl methanethiosulfonate (C) as fixed modifications, and oxidation (M) and phosphorylation (S, T, Y) as variable modifications. Peptides and proteins were filtered using ProteoIQ 2.7 (Premier Biosoft, Palo Alto, CA, USA) with strict peptide and protein probabilities, 0.8 and 0.95, respectively. For peptide confidence, we adopted the following cutoff values of Xcorr that are commonly used for the SEQUEST algorithm<sup>53</sup>: 2.31 for 2+, 2.41 for 3+, and 2.6 for 4+ peptides<sup>54</sup>. Peptide probability was applied to filter peptide assignments obtained from MS/MS database searching results using predictable false identification error rate (See Supplementary Table S2 for peptide information). To be differentially expressed with significance, a protein must have been quantified with a fold change >1.2 or <0.8, with at least three spectra in at least two of the biological quadruplicates, along with a Fisher's combined probability <0.05<sup>55</sup>. A protein is considered to be variable if it has an increase in expression in one component of the comparison and a decrease in the other; these variable proteins within biological replicates were excluded for further analysis. Functional analyses of proteins in biological process, molecular function, and cellular component were conducted using GO annotation (<http://www.geneontology.org/>) with Fisher's exact test based on false discovery rate ( $p$ -value ≤0.05)<sup>56</sup>. Blast2GO level 2–11 filtering was used to examine unique protein changes during comparison analysis. Accession numbers were compared between each genotype and treatment, and unique proteins were identified.

**Statistical analysis.** Differences in the MDA content, H<sub>2</sub>O<sub>2</sub> content and O<sub>2</sub><sup>-</sup> production rate were analyzed by one-way analysis of variance (ANOVA); if the ANOVA analysis was significant ( $P < 0.05$ ), Duncan's multiple range test was used to detect significant differences between groups.

## References

1. Tsuge, T. *et al.* Host-selective toxins produced by the plant pathogenic fungus *Alternaria alternata*. *FEMS Microbiol. Rev.* **37**, 44–66 (2013).
2. Brandwagt, B. F., Kneppers, T. J., Nijkamp, H. J. & Hille, J. Overexpression of the tomato *Asc-1* gene mediates high insensitivity to AAL toxins and fumonisin B1 in tomato hairy roots and confers resistance to *Alternaria alternata* f. sp. *lycopersici* in *Nicotiana glauca* plants. *Mol Plant Microbe Interact.* **15**, 35–42 (2002).
3. Grogan, R., Kimble, K. & Misaghi, I. A stem canker disease of tomato caused by *Alternaria alternata* f. sp. *lycopersici* [Fungus diseases]. *Phytopathol.* **65** (1975).
4. Clouse, S. D. & Gilchrist, D. G. Interaction of the *asc* locus in F8 paired lines of tomato with *Alternaria alternata* f. sp. *lycopersici* and AAL-toxin. *Phytopathol.* **77**, 80–82 (1987).
5. Du, L. *et al.* Biosynthesis of sphinganine-analog mycotoxins. *J Ind Microbiol.* **35**, 455–464 (2008).
6. Abbas, H. K. *et al.* Fumonisin- and AAL-toxin-induced disruption of sphingolipid metabolism with accumulation of free sphingoid bases. *Plant Physiol.* **106**, 1085–1093 (1994).
7. Riley, R. T., Norred, W. P. & Bacon, C. W. Fungal toxins in foods: recent concerns. *Annu. Rev. Nutr.* **13**, 167–189 (1993).
8. Xu, L. & Du, L. Direct detection and quantification of *Alternaria alternata* *lycopersici* toxins using high-performance liquid chromatography-evaporative light-scattering detection. *J Microbiol Methods.* **64**, 398–405 (2006).
9. Tsuda, K., Sato, M., Stoddard, T., Glazebrook, J. & Katagiri, F. Network properties of robust immunity in plants. *PLoS Genet.* **5**, 61–82 (2009).
10. Glazebrook, J. Contrasting mechanisms of defense against biotrophic and necrotrophic pathogens. *Annu Rev Phytopathol.* **43**, 205–227 (2005).
11. Zhang, L. *et al.* The involvement of jasmonates and ethylene in *Alternaria alternata* f. sp. *lycopersici* toxin-induced tomato cell death. *J. Exp. Bot.* **62**, 5405–5418 (2011).
12. Gadjev, I. Z., Hille, J. & Gechev, T. S. An extensive microarray analysis of AAL-toxin-induced cell death in *Arabidopsis thaliana* brings new insights into the complexity of programmed cell death in plants. *Cell. Mol. Life Sci.* **61**, 1185–1197 (2004).
13. Egusa, M., Ozawa, R., Takabayashi, J., Otani, H. & Kodama, M. The jasmonate signaling pathway in tomato regulates susceptibility to a toxin-dependent necrotrophic pathogen. *Planta* **229**, 965–976 (2009).
14. Li, L. *et al.* The tomato homolog of *CORONATINE-INSENSITIVE1* is required for the maternal control of seed maturation, jasmonate-signaled defense responses, and glandular trichome development. *Plant Cell* **16**, 126–143 (2004).
15. Dat, J. F. *et al.* Changes in hydrogen peroxide homeostasis trigger an active cell death process in tobacco. *Plant J.* **33**, 621–632 (2003).
16. Rao, M. V., Lee, H., Creelman, R. A., Mullet, J. E. & Davis, K. R. Jasmonic acid signaling modulates ozone-induced hypersensitive cell death. *Plant Cell* **12**, 1633–1646 (2000).
17. Zhang, A., Xu, T., Zou, H. & Pang, Q. Comparative proteomic analysis provides insight into cadmium stress responses in brown algae *Sargassum fusiforme*. *Aquat Toxicol.* **163**, 1–15 (2015).

18. Dai, S. J., Pang, Q. Y., Tian, Y. X., Chen, S. X. & Yan, X. F. Proteomic Analysis of Arabidopsis Leaves Subjected to Mechanical Wounding. *Curr. Proteomics* **12**, 124–136 (2015).
19. Tennant, J. R. Evaluation of the trypan blue technique for determination of cell viability. *Transplantation* **2**, 685–694 (1964).
20. Davey, M. W., Stals, E., Panis, B., Keulemans, J. & Swennen, R. L. High-throughput determination of malondialdehyde in plant tissues. *Anal Biochem* **347**, 201–207 (2005).
21. Torres, M. A., Dangel, J. L. & Jones, J. D. Arabidopsis gp91phox homologues AtrbohD and AtrbohF are required for accumulation of reactive oxygen intermediates in the plant defense response. *PNAS* **99**, 517–522 (2002).
22. Shinogi, T., Suzuki, T., Kurihara, T., Narusaka, Y. & Park, P. Microscopic detection of reactive oxygen species generation in the compatible and incompatible interactions of *Alternaria alternata* Japanese pear pathotype and host plants. *J Gen Plant Pathol.* **69**, 7–16 (2003).
23. Ogata, H. *et al.* KEGG: Kyoto Encyclopedia of Genes and Genomes. *Nucleic Acids Res.* **27**, 29–34(26) (1999).
24. Shi, Y. Mechanisms of caspase activation and inhibition during apoptosis. *Mol. Cell* **12**, 459–470 (2002).
25. Vartapetian, A. B., Tuzhikov, A. I., Chichkova, N. V., Taliansky, M. & Wolpert, T. J. A plant alternative to animal caspases: subtilisin-like proteases. *Cell Death Differ.* **18**, 1289–1297 (2011).
26. Solomon, M., Delledonne, M., Menachem, E., Levine, A. & Belenghi, B. The involvement of cysteine proteases and protease inhibitor genes in the regulation of programmed cell death in plants. *Plant cell* **11**, 431–443 (1999).
27. Czarny, P., Pawlowska, E., Bialkowska-Warzecha, J., Kaarniranta, K. & Blasiak, J. Autophagy in DNA damage response. *Int J Mol Sci.* **16** (2015).
28. Li, J., Brader, G. & Palva, E. T. Kunitz trypsin inhibitor: an antagonist of cell death triggered by phytopathogens and fumonisin B1 in *Arabidopsis*. *Mol. Plant* **1**, 482–495 (2008).
29. Mase, K. *et al.* Ethylene-responsive AP2/ERF transcription factor MACD1 participates in phytotoxin-triggered programmed cell death. *Mol Plant Microbe Interact.* **26**, 868–879 (2013).
30. Jia, C. *et al.* Multiple phytohormone signalling pathways modulate susceptibility of tomato plants to *Alternaria alternata* f. sp. *lycopersici*. *J. Exp. Bot.* **64**, 637–650 (2013).
31. DV, L. Enzymes of sphingolipid metabolism in plants. *Methods in Enzymol.* **311**, 130–149 (2000).
32. Wang, E., Norred, W. P., Bacon, C. W., Riley, R. T. & A H Merrill, J. Inhibition of sphingolipid biosynthesis by fumonisins. Implications for diseases associated with *Fusarium moniliforme*. *J Biol Chem.* **266**, 14486–14490 (1991).
33. Fuentes-Prior, P. & Salvesen, G. S. The protein structures that shape caspase activity, specificity, activation and inhibition. *Biochem. J.* **384**, 201–232 (2004).
34. Groover, A. & Jones, A. M. Tracheary element differentiation uses a novel mechanism coordinating programmed cell death and secondary cell wall synthesis. *Plant Physiol.* **119**, 375–384 (1999).
35. Klionsky, D. J. & Emr, S. D. Autophagy as a regulated pathway of cellular degradation. *Science* **290**, 1717–1721 (2000).
36. Dunn, J. *et al.* Peroxophagy: the selective autophagy of peroxisomes. *Autophagy* **1**, 75–83 (2005).
37. Shintani, T., Huang, W. P., Stromhaug, P. E. & Klionsky, D. J. Mechanism of cargo selection in the cytoplasm to vacuole targeting pathway. *Dev Cell* **3**, 825–837 (2002).
38. Hoerberichts, F. A. & Woltering, E. J. Multiple mediators of plant programmed cell death: interplay of conserved cell death mechanisms and plant-specific regulators. *Bioessays* **25**, 47–57 (2002).
39. Liang, H. *et al.* Ceramides modulate programmed cell death in plants. *Genes Dev.* **17**, 2636–2641 (2003).
40. Zhang, L. Regulation of tomato responses to *Alternaria alternata* f. sp. *lycopersici* and AAL-toxin by plant hormones. *Doctor Thesis, Zhejiang University* (2011).
41. Jong, A. J. d., Yakimova, E. T., Kapchina, V. M. & Woltering, E. J. A critical role for ethylene in hydrogen peroxide release during programmed cell death in tomato suspension cells. *Planta* **214**, 537–545 (2002).
42. Liu, L. *et al.* Ethylene independent induction of lycopene biosynthesis in tomato fruits by jasmonates. *J. Exp. Bot.* **63**, 5751–5761 (2012).
43. Mase, K. *et al.* Ethylene signaling pathway and MAPK cascades are required for AAL toxin-induced programmed cell death. *Mol Plant Microbe Interact.* **25**, 1015–1025 (2012).
44. Liang, W. *et al.* The Arabidopsis homologs of CCR4-associated factor 1 show mRNA deadenylation activity and play a role in plant defence responses. *Cell Res.* **19**, 307–316 (2009).
45. Elmore, J. M. & Coaker, G. The role of the plasma membrane H<sup>+</sup>-ATPase in plant-microbe interactions. *Mol Plant* **4**, 416–427 (2011).
46. Moore, T., Martineau, B., Bostock, R., Lincoln, J. & Gilchrist, D. Molecular and genetic characterization of ethylene involvement in mycotoxin-induced plant cell death. *Physiol Mol Plant Pathol.* **54**, 73–85 (1999).
47. Stefka, D., Spassievay, J. E. M. & Jacques Hille. The plant disease resistance gene *Asc-1* prevents disruption of sphingolipid metabolism during AAL-toxin-induced programmed cell death. *Plant J.* **32**, 561–572 (2002).
48. Filippou, P., Antoniou, C. & Fotopoulos, V. Effect of drought and rewatering on the cellular status and antioxidant response of *Medicago truncatula* plants. *Plant Signal Behav.* **6**, 270–277 (2011).
49. Zhou, Y., Zhang, Y., Zhao, X., Yu, H. & Shi, K., Yu, Jing. Impact of light variation on development of photoprotection, antioxidants, and nutritional value in *Lactuca sativa* L. *J. Agric. Food Chem.* **57**, 5494–5500 (2009).
50. Hurkman, W. J. & Tanaka, C. K. Solubilization of plant membrane proteins for analysis by two-dimensional gel electrophoresis. *Plant Physiol.* **81**, 802–806 (1986).
51. Vizcaino, J. A. *et al.* ProteomeXchange provides globally coordinated proteomics data submission and dissemination. *Nat Biotechnol* **32**, 223–226 (2014).
52. Shilov, I. V. *et al.* The Paragon Algorithm, a next generation search engine that uses sequence temperature values and feature probabilities to identify peptides from tandem mass spectra. *Mol Cell Proteomics.* **6**, 1638–1655 (2007).
53. Eng, J. K., McCormack, A. L. & Yates, J. R. An approach to correlate tandem mass spectral data of peptides with amino acid sequences in a protein database. *J Am Soc Mass Spectrom.* **5**, 976–989 (1994).
54. Jiang, X., Jiang, X., Han, G., Ye, M. & Zou, H. Optimization of filtering criterion for SEQUEST database searching to improve proteome coverage in shotgun proteomics. *BMC bioinformatics* **8**, 323 (2007).
55. Lury, D. A. & Fisher, R. A. Statistical Methods For Research Workers, London. *J R Stat Soc Ser C Appl Stat.* **21** (1972).
56. Conesa, A. *et al.* Blast2GO: a universal tool for annotation, visualization and analysis in functional genomics research. *Bioinformatics* **21**, 3674–3676 (2005).

## Acknowledgements

TA was a gift from Dr. Liangcheng Du (Department of Chemistry, University of Nebraska, Lincoln, NE, USA). This work was supported by the Ministry of Agriculture of China (2014ZX08009-003-001), Zhejiang Provincial Natural Science Foundation of China (LZ15C150001), and National Science Foundation of China (31171951, 30970244).

### Author Contributions

Q.W. and S.C. designed the research. M.Z. and H.L. performed tomato plant growth and toxin treatment. M.Z. and Z.S. performed cell death assays. M.Z. and S.H. performed the detection of H<sub>2</sub>O<sub>2</sub>, superoxide and MDA content. L.L. and M.Z. performed protein extraction and quantification, as well as iTRAQ labeling. J.K., C.P.D. and N.Z. performed iTRAQ LC-MS/MS data analysis. M.Z. and Q.M. wrote the article.

### Additional Information

**Supplementary information** accompanies this paper at <http://www.nature.com/srep>

**Competing financial interests:** The authors declare no competing financial interests.

**How to cite this article:** Zhang, M. *et al.* Critical Role of COI1-Dependent Jasmonate Pathway in AAL toxin induced PCD in Tomato Revealed by Comparative Proteomics. *Sci. Rep.* **6**, 28451; doi: 10.1038/srep28451 (2016).



This work is licensed under a Creative Commons Attribution 4.0 International License. The images or other third party material in this article are included in the article's Creative Commons license, unless indicated otherwise in the credit line; if the material is not included under the Creative Commons license, users will need to obtain permission from the license holder to reproduce the material. To view a copy of this license, visit <http://creativecommons.org/licenses/by/4.0/>